PHYSICAL REVIEW FLUIDS **2**, 013101 (2017)

Effect of pivot location and passive heave on propulsion from a pitching airfoil

A. W. Mackowski and C. H. K. Williamson
Department of Mechanical and Aerospace Engineering, Cornell University, Ithaca, New York 14853, USA
(Received 14 April 2016; published 4 January 2017)

We experimentally investigate the propulsive characteristics of a pitching NACA 0012 airfoil section, with emphasis on thrust and propulsive efficiency, at a Reynolds number of 1.7×10^4. For the sake of mechanical simplicity, we consider an airfoil restricted to a single actuator in the pitching direction. We examine the effect of changing the airfoil's axis of rotation, finding that contrary to Garrick's linear theory, there exists a pitching axis near the airfoil that maximizes propulsive efficiency. Next, we examine the effect of placing passive springs on the airfoil in the heave (transverse) direction using our Cyber-Physical Fluid Dynamics technique. This elastic heaving motion allows the airfoil to combine pitching and heaving modes while being actuated only in the pitching direction. Two sets of dynamics are considered: one case where the airfoil is weighted unevenly and pitched about its center of mass (so that the resulting heaving motion is independent of inertial forces), and another case where the airfoil's center of mass is fixed at its centroid. For pitching at an amplitude of 8° and a reduced frequency k of two, we find that elastic heave produces a maximum propulsive efficiency of 35%, compared to 25% without any heave motion. Further, while operating at the same efficiency as the static-pivot case, we find that passive heaving greatly increases the magnitude of the airfoil's thrust. The airfoil configurations with highest propulsive efficiency generally involve pitching near or ahead of the airfoil's leading edge.

DOI: 10.1103/PhysRevFluids.2.013101

I. INTRODUCTION

A. Motivation

For almost a century, oscillating airfoils have attracted interest as a means of propulsion, potentially to serve as a replacement in some circumstances for the ubiquitous rotating propeller. This view is encouraged by observations of nature, where certain fish and marine mammals can propel themselves, through movements of aerodynamically shaped fins, with surprising speed and agility.

While an airfoil section is a simplification of the form of a biological appendage, the fluid mechanics of thrust production retains many common features. Figure 1 shows the wake vortex dynamics produced by a pitching airfoil as it transitions from drag to net thrust production. This transition approximately corresponds to the onset of an inverse von Kármán vortex wake.

Promising results for oscillating-airfoil propulsion are found in a series of experiments by Anderson *et al.* [1], showing that one can achieve a steady-state propulsive efficiency of up to 87% for certain types of oscillation. Specifically, this high propulsive efficiency results from kinematics where the airfoil's heave (translation transverse to the flow) and pitch are both controlled. Interestingly, the propulsive efficiency of an airfoil undergoing only heaving motion is much lower; experiments by Heathcote and Gursul [2] and computations by Ashraf *et al.* [3] both result in efficiencies under 30% for Reynolds numbers on the order of 20 000. An airfoil undergoing pure pitching motion performs worse still, reaching only into the range of 10%–20% in flat-plate experiments by Buchholz and Smits [4] and NACA0012 section experiments by Mackowski and Williamson [5]. Clearly, the combination of heave and pitch movement is essential to efficient thrust production by the oscillating airfoil. Experimental studies such as Read *et al.* [6], and computations by Xiao and Liao [7], show that the effective angle of attack is an important parameter for propulsion; a sinusoidal angle of attack profile (created through specially controlled pitching and heaving motion) generally performs better than the profiles resulting from simple oscillatory heaving and pitching.

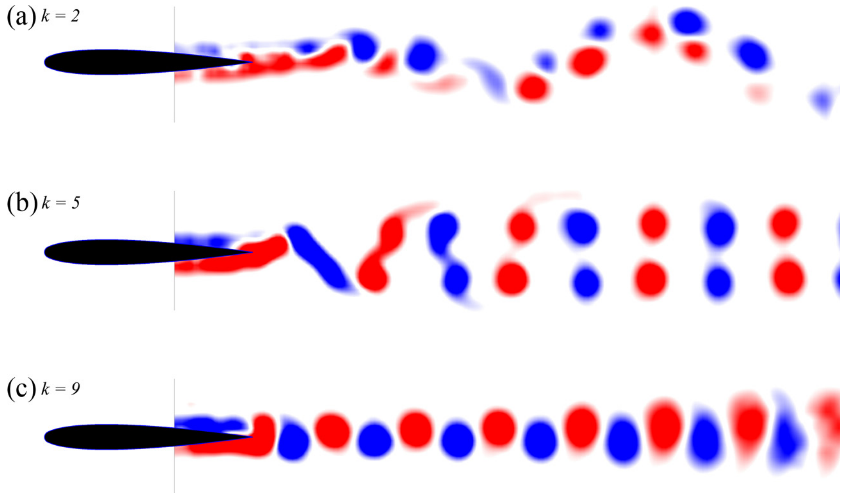

FIG. 1. Phase-averaged PIV measurements of vorticity in the wake of an airfoil pitching about its quarter-chord point. As the reduced frequency $k = 2\pi f c/2U_\infty$ is increased, we see different vortical arrangements in the wake.

As a matter of practicality for engineering applications, it would be advantageous to design a propulsive device with only a single degree of actuation, since having independent pitch and heave movement would be mechanically complicated. One approach would be to construct a mechanical linkage to allow a single motor to produce both pitch and heave motion, such as employed in the oscillating-airfoil energy extraction device by McKinney and DeLaurier [8]. However, a less mechanically involved approach is to introduce passive dynamics into the system in such a way that the combined active and passive motion is advantageous to propulsion. Following this idea, a current area of research is studying the propulsion of an airfoil with material flexibility.

Experiments by Heathcote and Gursul [2] find that a moderate amount of chordwise flexibility allows for more thrust production and can boost propulsive efficiency by up to 15% over a rigid foil. This conclusion confirms numerical simulations of a heaving, flexible airfoil performed by Miao and Ho [9], who find that an intermediate amount of flexibility benefits propulsion. At a Reynolds number of 10 000, the study produces a flexible configuration whose propulsive efficiency reaches 31%. Zhu [10] performs a series of inviscid simulations of airfoils with chordwise flexibility, claiming that this flexibility aids propulsive efficiency, but at the expense of decreased thrust. The consensus from the aforementioned studies is that a certain amount of chordwise flexibility in an airfoil section can increase its suitability for propulsion.

However, while flexible airfoils serve as good models for biomimetic propulsion, it is often difficult to quantify the exact physical properties that allow investigations to be reproduced elsewhere. In addition, for experimental investigations varying the amount of flexibility requires creating a new airfoil section and finding a new material; this greatly limits the ability of researchers to collect data for a large number of flexibility values.

Rather than looking at airfoil flexibility, an alternative approach to implementing passive dynamics is to impose a compliant fixture on a rigid airfoil. For example, we can attach an airfoil to a pivot with a rotational spring and impose a driving force in the heave direction. The airfoil is now free to rotate in the pitching direction under the influence of the fluid pressure and spring force acting upon it. Using a numerical simulation, Israeli [11] found modest gains in propulsive efficiency and thrust for this approach. Peng and Milano [12] experimentally investigate this system, though in the context of lift generation for flapping flight, making use of a force-feedback control system to implement the rotational spring.

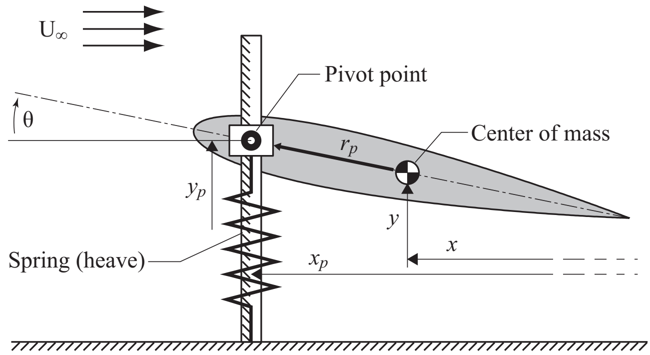

FIG. 2. Schematic of the airfoil configured for passive heave. Rotation is commanded at the pivot point, which is constrained to motion in the transverse (y) direction. A linear spring is attached to the foil at a location coincident with the pivot point.

Conversely to the previous dynamics, we can impose an oscillating pitching motion on the airfoil, but attach it to a linear spring in the heaving direction. Forces produced through the pitching motion create motion in the heaving direction as well, resulting in combined pitching and heaving. Murray and Howle [13] examine an inviscid model of these dynamics for several values of spring stiffness, finding that passive heave allows for positive net thrust generation at lower flapping frequencies. In the present study, we experimentally investigate this configuration to determine if passive dynamics can improve the thrust-generation properties of a pitching airfoil.

An advantage of the solid-body, elastic-fixture approach is that we can finely tune the system dynamics just by varying the spring constant. Additionally, we can rely on existing theoretical and computational tools for rigid oscillating airfoils to help analyze our results.

B. Terms and definitions

We command a pitching oscillation to the airfoil with frequency f_θ and amplitude θ_0, such that the airfoil's pitch angle is given by $\theta(t) = \theta_0 \sin(2\pi f_\theta t)$. As is common with oscillating airfoils, we express the flapping frequency nondimensionally as the reduced frequency k, defined as $k = 2\pi f_\theta c/2U_\infty$. Here c is the airfoil chord length and U_∞ is the free-stream velocity.

To characterize the airfoil's propulsive performance, we measure its thrust, power, and propulsive efficiency. Nondimensionally, we present these quantities as $C_T = \overline{F_x}/(\frac{1}{2}\rho U_\infty^2 cS)$, $C_P = \overline{P}/(\frac{1}{2}\rho U_\infty^3 cS)$, and $\eta = C_T/C_P$, respectively, where S is the span of the foil section.

When we investigate the effects of passive heave, the dynamical system we are imposing is shown in Fig. 2. We define the airfoil's mass ratio $m*$ as its weight relative to the weight of an equivalent volume of fluid. Rotational motion is commanded at a pivot point, located at a specified distance relative the leading edge. This pivot point is not always coincident with the airfoil's center of mass, which we will investigate at various positions. Locations on the airfoil centerline are defined by a distance p from the leading edge; a point at the trailing edge corresponds to $p/c = 1$. The pivot point is allowed to translate freely in the direction transverse to the flow, its height given as y_p. Finally, we attach a linear spring to the airfoil in the heave direction. While one could attach this spring at any point, for the sake of simplicity we keep its location coincident with the pivot point.

II. EXPERIMENTAL SETUP

A. Physical description

We perform our experiment in the Cornell-AFOSR hybrid water channel facility, which has a test section width of 38 cm and a maximum depth of 46 cm. For our airfoil section, we choose a NACA

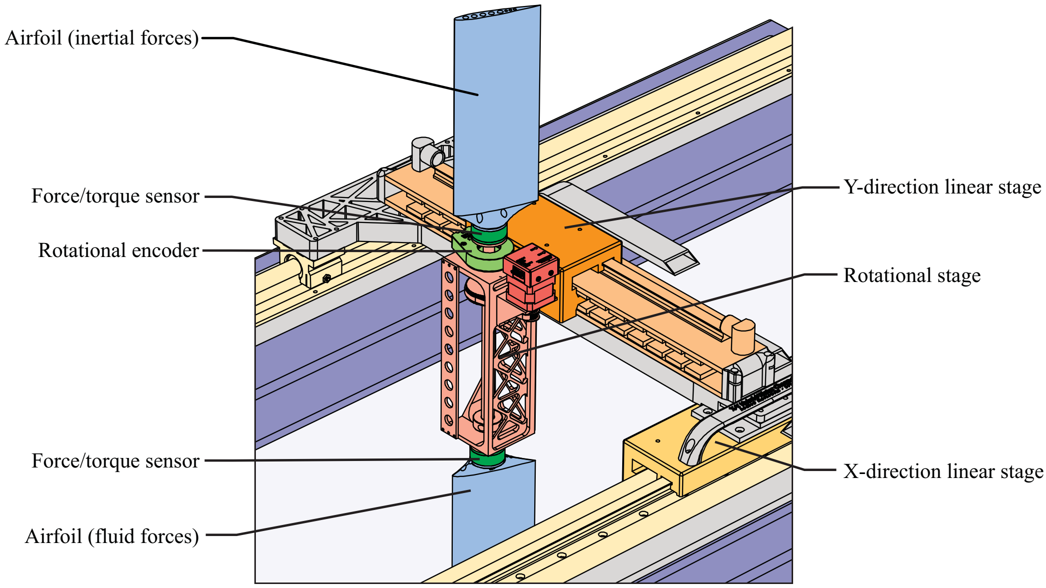

FIG. 3. Illustration of the Cornell-AFOSR “XYθ Flowing Tank.” High-performance linear actuators allow the airfoil section to translate in the streamwise and transverse directions, and a rotational stage allows for precise movement in the θ direction.

0012 profile with a chord length of 10 cm and a vertical submerged span of 24 cm. A horizontal endplate is positioned on the channel floor, resting just below the tip of the airfoil section, to limit three-dimensional end effects. Through all of the experiments presented here, the channel velocity is set to produce a chord-based Reynolds number of 16 600.

The water channel facility, illustrated in Fig. 3, is capable of producing motion in 3.5 degrees of freedom (channel speed, x translation, y translation, and θ rotation). The combination of freestream flow and x-y actuators gives it the qualities of both a water channel and a towing tank; we call it the Cornell-AFOSR “XYθ Flowing Tank.” We use high-performance, brushless linear actuators in the x and y directions to achieve precise motion with minimal phase delay. Although the rotational stage is aligned with the airfoil’s centroid, we employ motion in the x and y directions to produce rotation about any desired axis.

We measure fluid forces on the airfoil section with a three-axis force and torque transducer. An identical transducer and airfoil section are mounted inverted on the rotational stage, completely in air. These in-air measurements are calibrated and subtracted from the in-water measurements to separate inertial forces from fluid forces. Reported measurements are produced through ensemble averages of at least 30 experiments, which are required to produce sufficient precision in the face of sensor drift. Further information regarding the XYθ Flowing Tank and force measurement can be found in Mackowski and Williamson [5].

B. Implementation of passive heave dynamics

To investigate passive heave of the airfoil, we employ our Cyber-Physical Fluid Dynamics (CPFD) facility. CPFD employs a force-feedback control system that lets us impose arbitrary structural forces and moments. A control loop, running at 250 Hz, measures forces on the airfoil in real time. The control system removes forces due to the test object’s inertia, leaving behind a measurement of fluid forces. Next, we combine these fluid forces with software-defined, *virtual* forces; in this case, the virtual force is a linear spring in the transverse direction. The control system evaluates the combined impulse from the fluid and virtual forces over the sampling period, and then divides this impulse by a mass parameter (an arbitrary number, set in software, that determines the effective mass of the test object). The result is a velocity increment, ΔV, that is commanded to the actuator system.

This process repeats as movement creates fluid forces and fluid forces create movement. *The effect of the control system is to allow the airfoil to move in response to both a specified virtual spring force and physical fluid forces acting upon it, in real time.* A significant advantage of the CPFD approach is that the entire experimental process is completely automated. The spring constant, center of mass, and pivot point are all defined in software; entire 24-hr batches of experiments can be instructed and performed autonomously, with the control system responsible for changing the spring stiffness, zeroing forces, controlling the channel speed, and managing data files.

More details of the CPFD technique can be found in Mackowski and Williamson [14,15], including performance measurements and validation with purely physical experiments.

III. THEORETICAL TREATMENT

A. Source of linear theory

To further understand and predict the results of our pitching experiments, we turn to a theoretical investigation of the forces on an oscillating airfoil. Starting in the 1930s, Garrick [16] approached the problem of analyzing the propulsive performance of an airfoil oscillating at steady state in a fluid with a specified pitching amplitude, axis of rotation, heaving amplitude, and heaving phase. Garrick relied on the work of Theodorsen [17] to compute the unsteady lift forces on the airfoil and combined this with theory from von Kármán and Burgers [18] regarding forces in the streamwise direction. The fruit of Garrick's investigation is a closed-form (though elaborate) equation for the mean thrust and propulsive efficiency of the oscillating airfoil.

As one would expect, the linear theory in Garrick's work has several limitations; the equations are derived only for the small amplitude motion of a flat-plate airfoil. The flow is entirely inviscid and the vortex wake behind the airfoil is unable to deform. Surprisingly, even with these four restrictions, experimental measurements of unsteady fluid forces on a pitching airfoil by Mackowski and Williamson [5] show that linear theory produces quantitatively accurate predictions of the amplitude and phase of these forces, even at large pitching amplitudes and low Reynolds number. Results for the mean thrust, while qualitatively consistent, tend to overpredict the airfoil's performance.

Given that linear theory is a useful tool for predicting unsteady fluid forces on the airfoil, we would like to use it to predict the properties of an airfoil undergoing passive motion, specifically, controlled pitching with a linear spring in the transverse direction. However, calculating fluid forces from theory requires knowing the exact heave amplitude and phase relative to pitching, both of which are unknown before the experiment. This problem has long been recognized in the theory of airfoil flutter, where Theodorsen's technique is sometimes used as a fluid model for an elastically mounted airfoil [19]. Before the advent of modern state-space control design, one common approach was to approximate the fluid theory with a rational transfer function, then use frequency-domain analysis to calculate the amplitude response of the combined passive system (see Ref. [20], which includes a thorough overview of Theodorsen's model in the context of control design). In a numerical study of oscillating-foil propulsion using spring-mounted actuators, Harper *et al.* [21] use a third-order approximation of Theodorsen's model to simulate fluid forces. The authors take advantage of this approximation by using it to examine the stability properties of their coupled fluid-structure system, a task which is difficult with a more complex fluid model.

B. Derivation of constraints for fluid forces

For the present work, we will instead solve the coupled fluid-structure system directly, using the full form of the Theodorsen's fluid theory. Treating this fluid model as a "black box," we use equations arising from the complete system dynamics to place constraints on the amplitude and phase of the y-direction fluid force for a given oscillation frequency. The first step is solving for the airfoil's steady-state heave amplitude and phase, giving us full knowledge of its kinematics. With this information, we can in turn produce the airfoil's mean thrust and propulsive efficiency from Garrick's equations. Using the system depicted in Fig. 2, we can write the y-direction dynamics about the center of mass as

$$m\ddot{y} = F_{fl} - K(y + r_P \sin\theta)\,.$$

Here y is the elevation at the center of mass, F_{fl} is the fluid force acting on the foil in the y direction, K is the spring constant, and r_p is the distance from the center of mass to the pivot point. We can produce the dynamics about the pivot point y_p by using the relation $y_p = y + r_p \sin\theta$ with a small-angle approximation (assuming a small pitching amplitude, we have $y_p \approx y + r_p\theta$).

$$m(\ddot{y}_p - r_p\ddot{\theta}) = F_{fl} - K y_p\,.$$

We impose a rotational motion on the airfoil defined as $\theta(t) = \theta_0 \sin(\omega t)$. Additionally, we make the assumption that both the heave amplitude and fluid force oscillate sinusoidally at steady state. This entails defining the heave motion as $y_p = h_0 \sin(\omega t - \phi)$, where h_0 is the heave amplitude and the heaving phase ϕ represents a lag behind $\theta(t)$. Finally, the fluid force is postulated as $F_{fl} = F_0 \sin(\omega t - \psi)$. Substituting these relations into the overall system dynamics, we obtain

$$-mh_0\omega^2 \sin(\omega t - \phi) + mr_p\theta_0\omega^2 \sin(\omega t) = F_0 \sin(\omega t - \psi) - Kh_0 \sin(\omega t - \phi)\,.$$

Because the overall phase is arbitrary, we can shift the absolute phase of the previous equation forward by ϕ; upon rearranging, we have

$$\left(\frac{K}{m} - \omega^2\right)h_0 \sin(\omega t) = -r_p\theta_0\omega^2 \sin(\omega t + \phi) + \frac{F_0}{m}\sin(\omega t - \psi + \phi)\,.$$

Expanding the above equation using the sum-of-angles identity, we arrive at

$$\begin{aligned}\left(\frac{K}{m} - \omega^2\right)h_0 \sin(\omega t) = &- r_p\theta_0\omega^2 \cos\phi \sin\omega t - r_p\theta_0\omega^2 \sin\phi\cos\omega t \\ &+ \frac{F_0}{m}\cos(\phi - \psi)\sin\omega t + \frac{F_0}{m}\sin(\phi - \psi)\cos\omega t\ .\end{aligned}$$

Matching terms of $\sin\omega t$ and $\cos\omega t$, we now have two constraint equations on the system dynamics:

$$\left(\frac{K}{m} - \omega^2\right)h_0 = -r_p\theta_0\omega^2\cos\phi + \frac{F_0}{m}\cos(\phi - \psi)\,, \tag{1}$$

$$0 = -r_p\theta_0\omega^2\sin\phi + \frac{F_0}{m}\sin(\phi - \psi)\,. \tag{2}$$

For Eq. (1), we will introduce the frequency ratio $f^* = f_\theta/f_n = \omega/\sqrt{K/m}$, giving

$$h_0\omega^2(f^{*-2} - 1) = -r_p\theta_0\omega^2\cos\phi + \frac{F_0}{m}\cos(\phi - \psi)\,. \tag{3}$$

C. Numerical solution to constraint equations

The next step in analyzing the performance of the passive-spring system is to apply the constraint equations derived above to a fluid force model; in our case, we are using the linear theory derived by Theodorsen. The simplest way of achieving this is to produce a map of the unsteady fluid force in the heave phase-amplitude space, as shown in Fig. 4. With this information, one can numerically compute contours representing solutions of the above constraint equations (1) and (2).

However, for the case of fixed reduced frequency (i.e., constant f_θ), a faster and more precise method of generating predictions is as follows. First, distribute N points spanning the space of heaving phase ϕ. For each value of ϕ, numerically iterate on the fluid model to find a heave amplitude h_0 that satisfies constraint equation (2), if such a solution exists. It is observed (for the linear fluid theory)

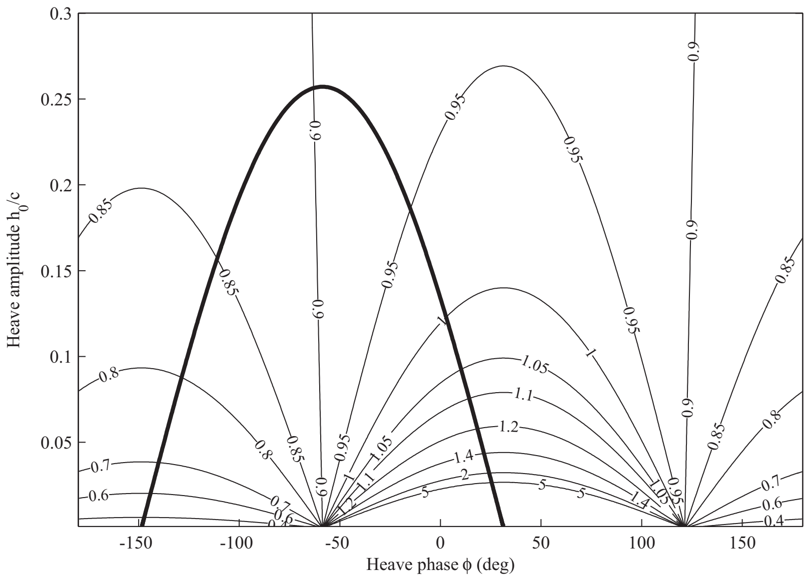

FIG. 4. Map of heave phase and amplitude used for predicting the response of the passive-heave system: in this case, pitching with the center of mass at the airfoil's centroid, pivot point at the quarter-chord, mass $m^* = 40$, and reduced frequency $k = 2$. The bold line indicates points where the fluid force predicted by Theodorsen's analysis satisfies constraint equation (2). The remaining contours indicate levels of frequency ratio f^* computed from constraint equation (3).

that for a fixed value of ϕ, the value of the right-hand side of constraint equation (2) is monotonic with h_0 (this parameter is used indirectly to compute the fluid force). Therefore, this iteration step can be quickly and efficiently solved by a standard one-dimensional zero-finding algorithm. Finally, for each solution discovered for constraint equation (2), one computes the corresponding frequency ratio f^* using equation (3).

The resulting tuples of f^*, h_0, and ϕ represent heaving and pitching kinematics that satisfy both the system dynamics and the fluid force model. The final step is to insert these parameters into the equations of Garrick to determine the airfoil's thrust and propulsive efficiency. It is relevant to note that this method for determining the passively-mounted airfoil's performance is extremely computationally efficient, even compared to inviscid panel methods. Evaluating fluid forces from linear theory is a single algebraic computation, and computing the frequency response of the full dynamical system only requires a set of iterations on one-dimensional, monotonic functions.

D. Comparison with existing computational work

We can compare the results of our theoretical predictions for a passive-heave system with the computational work of Murray and Howle [13], who approach the same problem using an unsteady, two-dimensional vortex lattice method. While our present experimental investigation maintains a fixed oscillation frequency while varying the system's natural frequency, Murray and Howle examine three fixed choices of spring stiffness $K^* = K/\frac{1}{2}\rho U_\infty^2$ as the oscillation frequency is varied. However, for the sake of comparison we modified our current numerical technique to produce predictions under the same conditions.

Figure 5 shows calculations of the airfoil's heave amplitude, predicted using the method of Murray and Howle and from the current technique. We see reasonable agreement between the two sets of calculations, especially given the simplicity of the linear-theory approach. For the airfoil's thrust and efficiency, both methods show the same qualitative trends, though the linear theory consistently overestimates the magnitude of thrust on the airfoil.

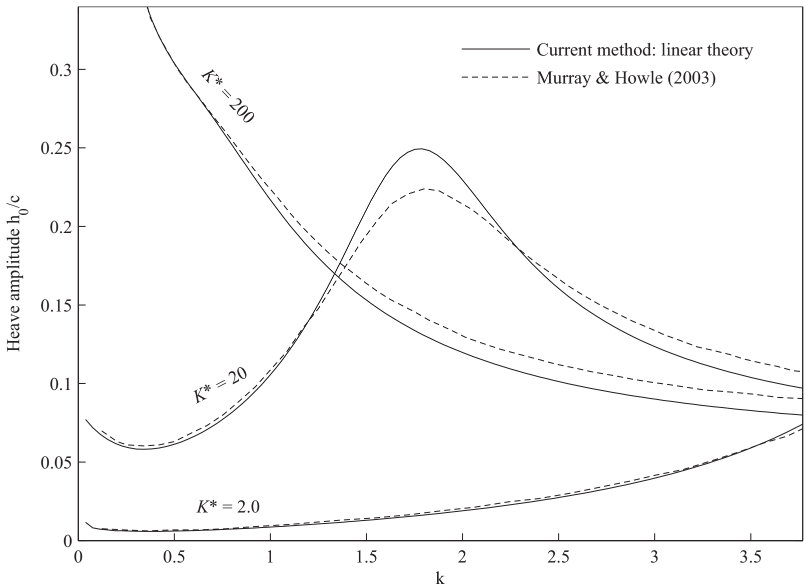

FIG. 5. Heave amplitude h_0/c versus oscillation frequency k for a passive-heave airfoil with fixed spring stiffness. The plot compares results from the vortex lattice method of Murray and Howle with predictions using linear theory in the current technique ($m* = 1$, $\theta_0 = 15^\circ$).

IV. MEASUREMENTS FOR PITCHING WITH STATIC PIVOT POINT

Before investigating the effects of passive heave on a pitching airfoil, it is useful to examine the airfoil's performance without any heave movement. We call this the *static-pivot* case. From Mackowski and Williamson [5], we know that for an airfoil pitching about its quarter-chord point with an amplitude of 8°, the maximum propulsive efficiency remains under 15% across all pitching frequencies tested. However, we need not be limited by pitching about the quarter-chord point; one could induce simple pitching motion at any point on or outside of the airfoil's body.

As we move the pivot point further from the airfoil's body (ahead of the leading edge, or behind the trailing edge), the motion of the airfoil becomes more and more like heaving; translational velocities have similar values along the airfoil section. We know from experiments (e.g., Ref. [2]) and linear theory that heaving motion has the potential for higher propulsive efficiency than pure pitching. Therefore, it stands to reason that one might find the best propulsive performance when oscillating at a point far removed from the airfoil body.

We show in Fig. 6 a plot of the airfoil's thrust coefficient versus the pivot point, keeping constant the pitching amplitude and frequency. As expected, the thrust increases as we move the pitching point further from the airfoil body. The airfoil produces a minimum amount of thrust when pitching near the three-quarter chord point, in agreement with linear theory. We also note an asymmetry in thrust production with respect to this minimum point; the airfoil fares better pitching relative to an upstream point than a downstream point. In the former case, the airfoil's trailing edge has a larger tangential velocity than its leading edge, the effect of which perhaps reduces the strength of leading-edge vortices that interfere with thrust production.

According to linear theory, the airfoil's propulsive efficiency should increase monotonically with the pitching axis' distance from the airfoil body, as was the case with thrust. Figure 7 shows measurements of the airfoil's propulsive efficiency at the same conditions as before. We have included calculations from linear theory, to which we have added a quasisteady drag coefficient computed from averaging the airfoil's static drag over the pitch angles encountered during a cycle of

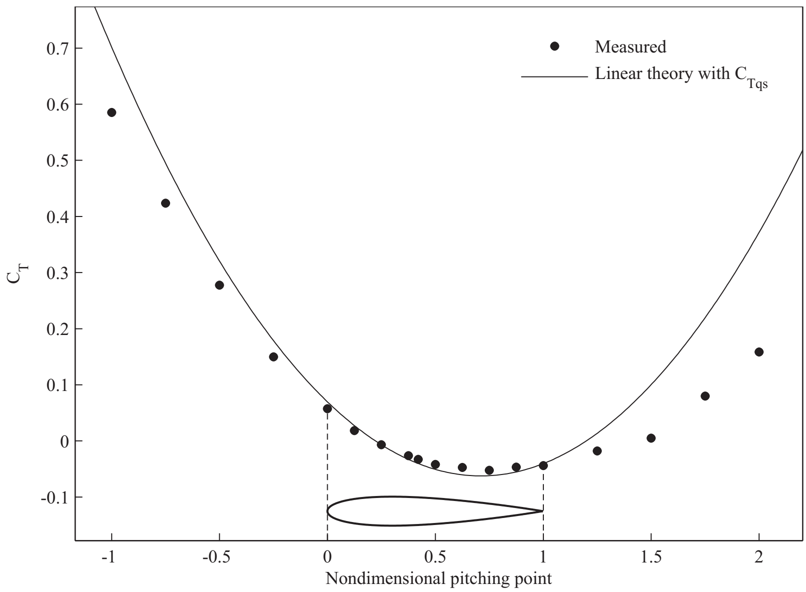

FIG. 6. Thrust coefficient for the airfoil oscillating at a constant reduced frequency $k = 2$ and pitching amplitude $\theta_0 = 8^\circ$, plotted against the location of the pitching axis. For comparison, we plot the prediction from linear theory (with the airfoil's quasistatic drag coefficient added).

oscillation. From this plot, we immediately notice that contrary to the trend in the fluid theory, the airfoil's propulsive efficiency peaks at an upstream pitching axis of about a half-chord length from the leading edge.

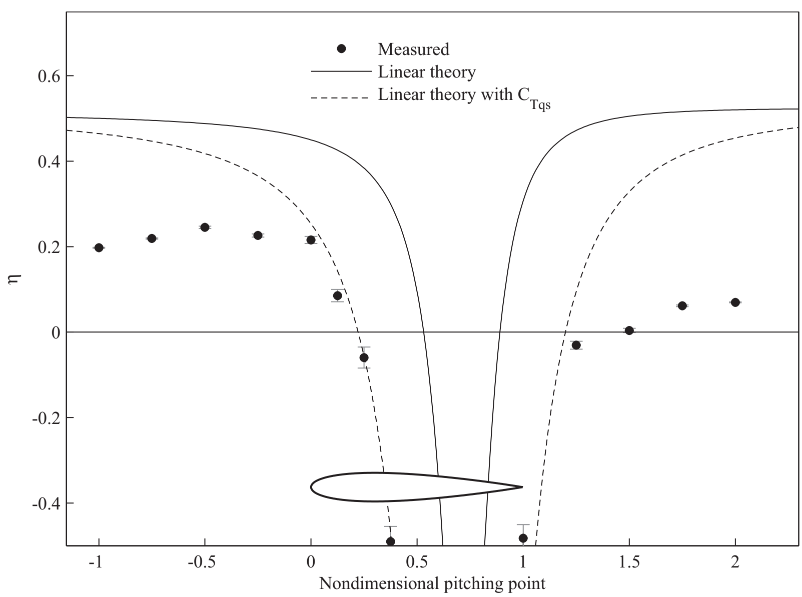

FIG. 7. Propulsive efficiency for the airfoil pitching at reduced frequency $k = 2$ and amplitude $\theta_0 = 8^\circ$, plotted against the location of the pitching axis. For comparison, we have included the prediction from linear theory with and without an added quasistatic drag component.

At this optimal location, we observe a propulsive efficiency of 25% and a thrust coefficient of 0.28. With both a reasonable thrust and efficiency, pitching about this point is suitable for propulsion, much more so than pitching about the airfoil's quarter-chord point. Interestingly, pitching around the optimum point (at the current frequency) results in a trailing-edge Strouhal number $\mathrm{St}_A = 0.27$, which is consistent with optimal thrust production in previous oscillating-foil propulsion studies (for example, Triantafyllou *et al.* [22] find optimal performance between St_A values of 0.25 and 0.35, while Buchholz and Smits [4] find an optimal range between 0.125 and 0.34).

V. MEASUREMENTS FOR PITCHING WITH PASSIVE HEAVE

While we can achieve reasonable thrust and efficiency by pitching statically at a point upstream of the airfoil's leading edge, we seek to determine if one can improve these characteristics by allowing the airfoil to heave passively. As there are too many independent parameters to study exhaustively, we restrict our investigation to the case of pitching with a reduced frequency $k = 2$, a pitch amplitude $\theta_0 = 8^\circ$, and a nondimensional mass $m^* = 40$. To vary the frequency ratio f^*, we modify the stiffness of the spring in the heaving direction while keeping the pitch oscillation frequency constant.

Our fixed choices for k and θ_0 are designed to produce an intermediate range of thrust over a variety of experimental conditions. This value of pitching frequency k is small enough that the airfoil needs additional heaving motion to perform well, but large enough to generally provide positive net thrust. Likewise, our choice of pitching amplitude θ_0 is small enough that we can reasonably compare it with linear theory, yet large enough to produce sufficient thrust. The nondimensional mass parameter is set close to the lowest value that our CPFD apparatus allows. For practical applications, however, the nondimensional mass of the propulsive foil might be closer to 1.

A. Pivoting about the airfoil's center of mass

In this set of experiments, we operate in a simplified configuration where the airfoil's center of mass is coincident with its pivot point. This scenario corresponds to weighting the airfoil unevenly and is special because any resulting heaving motion is solely due to fluid forces (pitching about the center of mass produces no inertial heaving forces). We examine the effects of spring stiffness on the airfoil's thrust and efficiency at six pitching locations: one chord length ahead of the leading edge ($p/c = -1$), at the leading edge ($p/c = 0$), at the quarter-chord point ($p/c = 0.25$), at the centroid ($p/c = 0.42039$), at the trailing edge ($p/c = 1$), and one chord length behind the trailing edge ($p/c = 2$).

The complete performance data for the various pitching configurations is shown in Fig. 8. We can see that passive springs are of little benefit when the airfoil is weighted at its centroid or quarter-chord point; these configurations are never able to produce positive net thrust at the present oscillation frequency. Pitching about the leading edge fares marginally better, producing a propulsive efficiency that consistently stays just below 20%, though the magnitude of thrust produced is still relatively small.

The most promising configurations for passive pitching about the center of mass occur when pitching about a location removed from the airfoil body. When pitching about a location one chord length ahead of the leading edge, we see a maximum propulsive efficiency of 30%, corresponding to a thrust coefficient of 0.23. Conversely, by weighting the airfoil one chord length behind the trailing edge, we can achieve a maximum propulsive efficiency of 35% while producing significant thrust ($C_T = 0.24$).

The thrust production of several foil configurations is plotted as a function of frequency ratio f^* in Fig. 9. For pitching one chord length ahead of the leading edge ($p/c = -1$), we find that passive springs do not produce a benefit for net thrust; the maximum thrust produced by the airfoil is only marginally higher than for pitching without heave (i.e., $f^* = 0$). However, for pitching one chord length behind the trailing edge, we see a dramatic increase in thrust enabled by the passive dynamics. While pitching with a static pivot point in this configuration produces a thrust coefficient

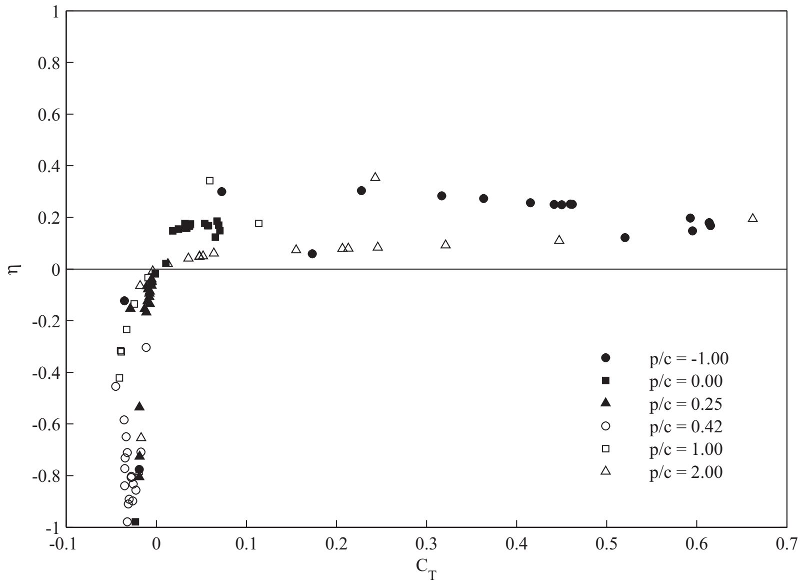

FIG. 8. Collected measurements of thrust and efficiency for the airfoil pitching about its center of mass, shown for various center-of-mass locations and spanning multiple values of frequency ratio f^*. The highest measured propulsive efficiency is 35%, corresponding to an airfoil with a hypothetical weight distribution one chord length behind the trailing edge.

of 0.16, adding springs in the heave direction allows the system to produce up to four times as much thrust. However, once the frequency ratio surpasses unity, the thrust gains produced by passive heave vanish. It should be noted that in all of the configurations tested, allowing the system to translate

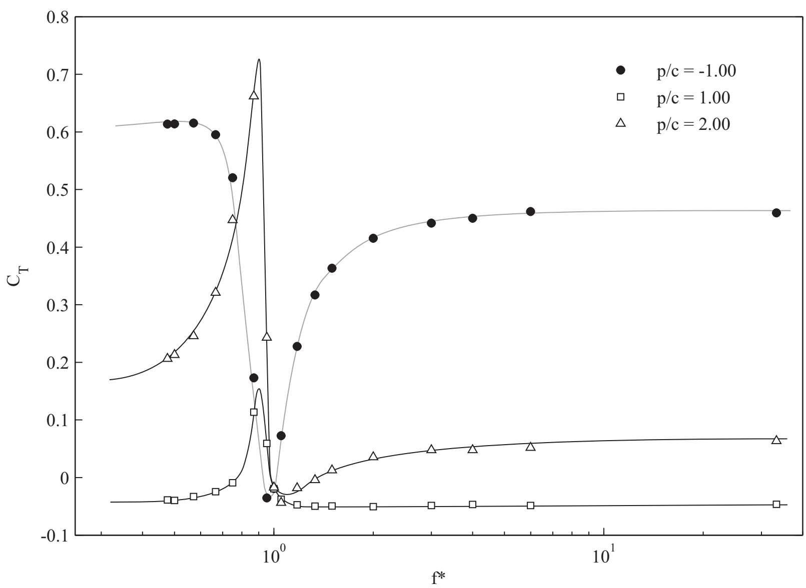

FIG. 9. Thrust production versus frequency ratio for an airfoil pitching about its center of mass. Values are shown for airfoils weighted in three locations: one chord length ahead of the leading edge, the trailing edge, and one chord length behind the trailing edge.

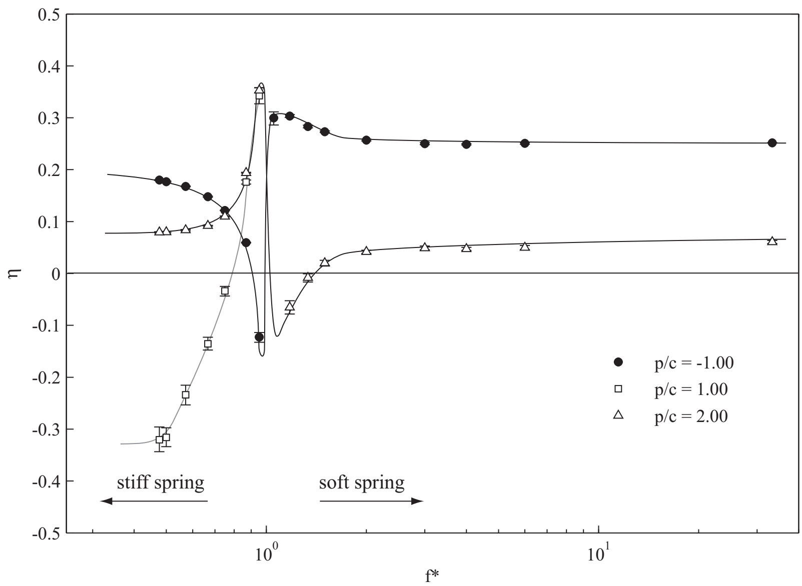

FIG. 10. Propulsive efficiency versus frequency ratio for airfoils pitching about their center of mass. Error bars show a 95% confidence interval for the measurements. For the case of pitching about the trailing edge ($p/c = 1$), the propulsive efficiency decreases below the limits of the plot beyond $f^* = 1$.

freely in the heave direction ($f^* \to \infty$) never produced an improvement in thrust over the baseline, static-pivot scenario.

In terms of propulsive efficiency, Fig. 10 shows an interesting comparison between the pivot locations chosen in Fig. 9. For pitching one chord length ahead of the leading edge, efficiency is improved relative to the baseline case by employing a "soft" spring in the heave direction, where the system's natural frequency is below the pitching frequency. For this pivot location, we see a wide region of frequency ratio f^*, from 1.05 to infinity, with propulsive efficiency greater than 25%. However, for a system with stiff springs ($f^* < 1$), we see a significant drop in propulsive efficiency from the static-pivot case. Allowing the pivot point to translate freely without springs ($f^* \to \infty$) represents an improvement in efficiency over the static-pivot case (25% vs 20%).

Conversely, pitching one chord length behind the trailing edge tends to perform best with stiff springs. By allowing passive heave, we see a drastic increase in propulsive efficiency from 7% with the static-pivot scenario to 35% at a frequency ratio $f^* = 0.95$. With softer springs, though, the frequency ratio passes unity, and the system achieves worse efficiency than the static-pivot case.

B. Pivoting with the airfoil's center of mass at its centroid

After examining a series of configurations where the airfoil is weighted to change its center of mass location, we now explore a different set of dynamics. Here, keeping the airfoil's center of mass fixed at its centroid (as if the airfoil is made of a uniform-density material), we examine the effect of varying the location of an independent pivot point. For our NACA 0012 airfoil, the centroid is located at a normalized length $p/c = 0.42039$ from the leading edge. Unlike the previous system, in the absence of fluid forces the airfoil will heave when pitched due to its own inertia.

The performance data for all the airfoils tested under this configuration are shown in Fig. 11. We can quickly see that by separating the pitching point from the airfoil's centroid, we achieve a much higher amount of thrust production, reaching a maximum C_T of 1.29. This value is almost twice the maximum thrust for the previous configuration, where the center of mass and pivot point are coincident. While the maximum propulsive efficiency here is somewhat

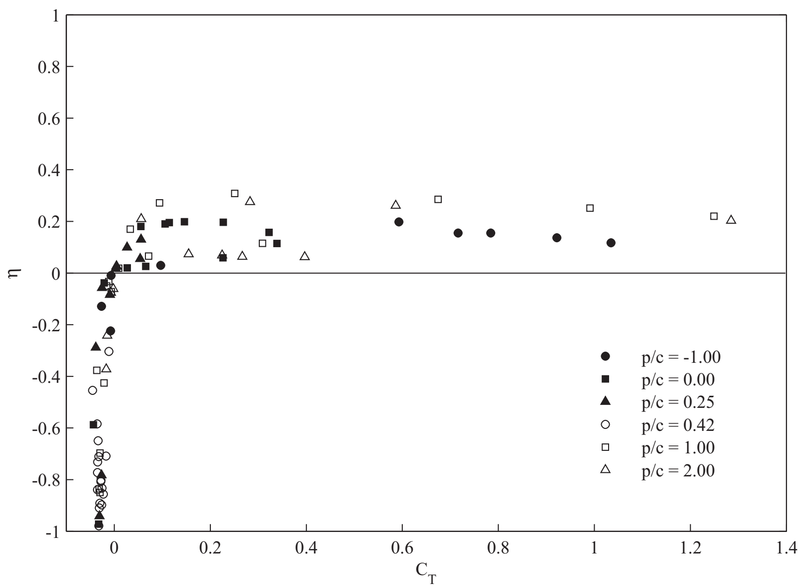

FIG. 11. Plot of thrust and efficiency for all airfoil configurations tested (the pivot point is varied while the center of mass remains at the centroid). The best measured value of propulsive efficiency is 31%, with a thrust coefficient of 0.25, corresponding to an airfoil pitching about its trailing edge.

less than the previous investigation (31% versus 35%), the overall performance is improved; for example, the weighted-airfoil configuration could produce a C_T of 0.66 at 19% efficiency, while the current configuration can produce the same amount of thrust at 29% propulsive efficiency.

Of all the pitching locations tested, Fig. 11 indicates that the best performance is achieved when pivoting at the trailing edge, closely followed by pivoting one chord length behind the trailing edge. The trailing-edge pivot location was able to produce an extremely wide range of thrust (up to about 23 times the airfoil's quasistatic drag) all while maintaining propulsive efficiency between 22% and 31%.

In Fig. 12 we can see the airfoil's thrust coefficient plotted against frequency ratio for selected cases of pivot location. With a frequency ratio f^* greater than about 3, none of the configurations tested were able to produce significant thrust. Peak thrust production is achieved near a frequency ratio of unity, and all of the passive-heave configurations are able to significantly exceed their static-pivot thrust. Pitching a chord length behind the trailing edge produces thrust in a wider range of reduced frequency than pitching at the trailing edge.

Although passive dynamics allow the airfoil with a pre-leading-edge ($p/c = -1.0$) pivot to produce more thrust than the static-pivot case, Fig. 13 shows that they simultaneously decrease the system's propulsive efficiency. For this pivot location, there is no benefit to using springs in the heave direction; one would be better suited with a static pivot located further ahead of the airfoil's leading edge.

However, for the airfoils pitching about the trailing edge and a chord length beyond the trailing edge, springs in the heave direction greatly assist the system's propulsive efficiency. By using slightly soft springs (f^* just greater than unity), these two airfoils reach peak propulsive efficiencies of 31% and 28%, respectively. For the airfoil pitching about the trailing edge, this high value of efficiency is striking; with a static pivot, the airfoil was not even capable of producing net thrust. This airfoil configuration benefits from a measured amount of spring compliance, where a spring that is either too stiff or too soft causes it to fall off the favorable regions of thrust and efficiency.

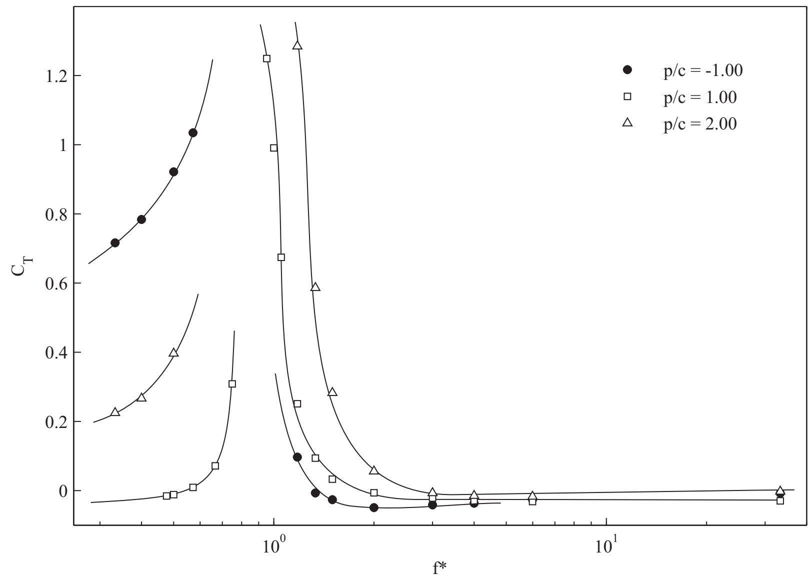

FIG. 12. Plot of thrust versus frequency ratio for a constant-density airfoil, shown for three pitching locations: one chord length ahead of the leading edge, trailing edge, and one chord length behind the trailing edge. Around a frequency ratio of 1, the fluid forces were so large that they exceeded the limits of the measurement hardware.

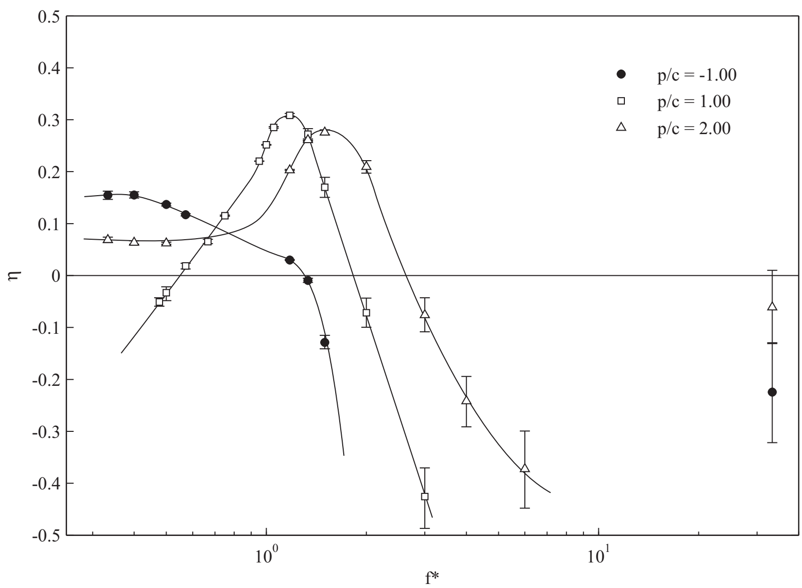

FIG. 13. Propulsive efficiency plotted against frequency ratio for several pivot locations, with the airfoil's center of mass fixed at the centroid. For the airfoil pitching ahead of the leading edge, efficiency tends to decrease from its static-pivot value. However, the airfoils pitching at the trailing edge and behind the trailing edge reach peak efficiency at frequency ratios of 1.18 and 1.50, respectively.

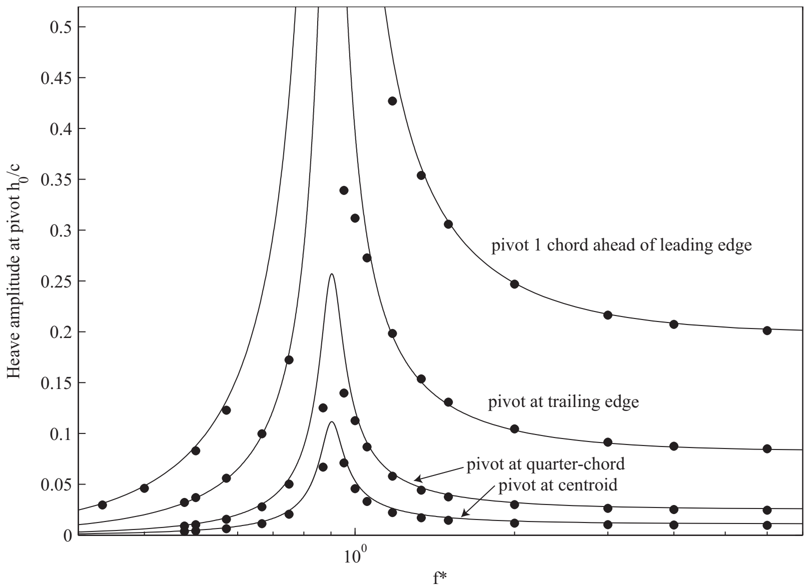

FIG. 14. Comparison between measured heave amplitudes and predictions from linear theory (solid lines) for the constant-density airfoil with passive dynamics. While one might not expect linear theory to be applicable, it is remarkably accurate in predicting the airfoil's measured heave amplitude.

VI. ANALYSIS AND COMPARISON

A. Performance increase due to passive heave

For pure pitching at 8° amplitude and a reduced frequency $k = 2$, Fig. 7 shows that peak propulsive efficiency for our NACA 0012 airfoil is 25%, with a corresponding thrust coefficient of 0.28. When we include passive dynamics, we can produce over twice as much thrust while simultaneously operating at 29% propulsive efficiency. Our absolute maximum propulsive efficiency at these pitching conditions is 35% at a thrust coefficient of 0.24, representing a sizable improvement over the static-pivot scenario.

B. Applicability of linear theory

We find that linear theory is a useful tool for analyzing different pitching configurations. Figure 14 shows several predictions made using the technique discussed in Sec. III for the airfoil's heave amplitude. We find that while our experiment violates all of the assumptions underlying the linear theory (flat-plate airfoil, infinite Reynolds number, small amplitude of motion, and nondeforming vortex wake), the theory nevertheless produces quantitatively accurate kinematic predictions for all of the passive-dynamics scenarios we have considered. However, we do notice that as heave amplitudes increase beyond about $h_0/c = 0.3$, the accuracy of the predictions suffers, likely due to significant flow separation on the airfoil.

Although the linear theory of Theodorsen provides good estimates of the airfoil's kinematics in the heaving direction, the component of the theory in the streamwise direction, due to von Kármán and Burgers, fares less consistently well with quantitative predictions. We see a reasonable agreement between theory and experiment for thrust, shown in Fig. 6, for the present reduced frequency and pitching amplitude. Figure 15 shows a comparison of propulsive efficiency for several passive-heave configurations; while streamwise linear theory captures the general trend when quasistatic drag is added in, measured values of efficiency still fall well short of their predicted peaks.

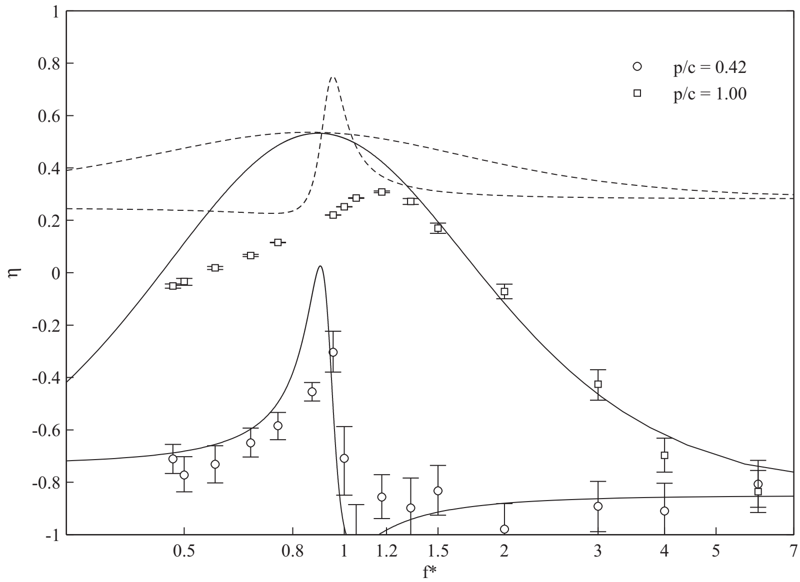

FIG. 15. Propulsive efficiency for the airfoil with constant density, shown for two pivot locations. Dashed lines indicate raw predictions from linear theory, while solid lines represent an inference from linear theory with the airfoil's quasistatic thrust C_{Tqs} added in.

C. Pitching at resonant frequency

One of the most basic questions about the effect of passive heaving is whether or not operating at the system's natural frequency ($f^* = 1$) produces a thrust-generating excitation. There are two outcomes that seem equally plausible: (1) the fluid system couples constructively with the springs forces, building up to a large heaving motion (highly excited) or (2) the extra degree of freedom provided by the heave axis allows the system to relax into a state that minimizes power transfer to the fluid (minimally excited). In fact, we find both of these outcomes in our experiment.

For the airfoil pitching about its center of mass, operating at $f^* = 1$ allows the airfoil to expend a trivial amount of power, as shown in Fig. 16. As predicted by linear theory, when the frequency ratio approaches unity we see a drastic cutoff in the power required to pitch the airfoil at the specified amplitude and frequency. This phenomenon is exhibited for all center-of-mass locations. Interestingly, the net thrust at $f^* = 1$ does not represent the system's minimum thrust (maximum drag); instead it converges to the airfoil's static profile drag coefficient $-C_{D0} = -0.032$ for all cases (this is different, and larger than, the system's quasistatic thrust coefficient $C_{Tqs} = -0.054$).

This last point corroborates visual observations of the channel surface. Typically, thrust-producing oscillations create dimples on surface corresponding to powerful vortices in the airfoil's wake (see Fig. 1). However, when oscillating at $f^* = 1$, the channel surface remains perfectly flat. This observation hints that the airfoil is oscillating in a way that is minimizing its generation of a vortex wake.

To further understand this scenario, we can examine the kinematics that result from the combination of pitching motion with passive heave. Although we command rotation about a specified pivot point, the addition of heaving motion can change the airfoil's apparent axis of rotation, depending on the heave phase and amplitude. In his theoretical study of oscillating-foil propulsion, Lighthill [23] notes that changing the phase between heaving and pitching is equivalent to displacing the airfoil's pitching axis. Although that result is valid only for small angles, we generalize it by defining the airfoil's *effective* pitching point, p_e, as the locus where the total translational excursion during one oscillation cycle is minimized. In other words, the effective pitching point is the axis where pitching and heaving are minimally coupled.

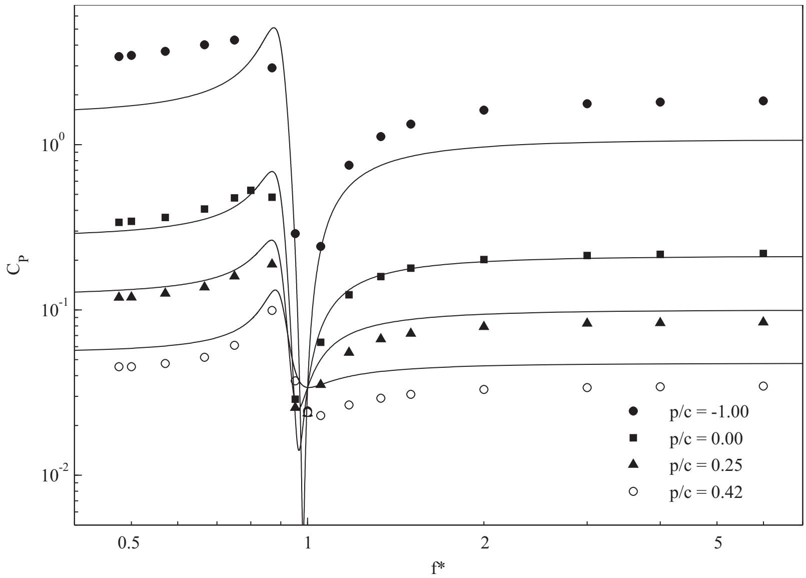

FIG. 16. Power coefficient for the airfoil pitching about its center of mass, shown for several center-of-mass locations. The solid lines represent predictions from linear theory. Note that for $f^* = 1$, all of the configurations share the same power coefficient.

The airfoil's calculated effective pivot point is shown in Fig. 17 for pitching about various center-of-mass locations (i.e., the unevenly weighted airfoil). For these configurations, there is no heaving movement due to the airfoil's inertial forces. At low values of f^*, where the high spring forces prevent significant heaving movement, the effective pitching point tends towards the airfoil's specified pivot location. Interestingly, at $f^* = 1$, we find that the nondimensional effective pitching

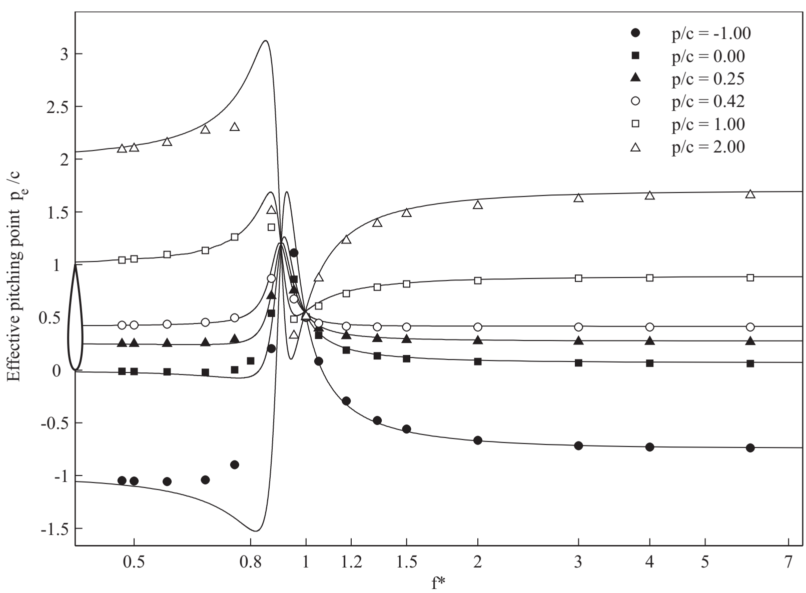

FIG. 17. Nondimensional effective pivot point p_e/c for airfoils pitching about their center of mass. Measurements are in good agreement with predictions from linear theory (solid lines).

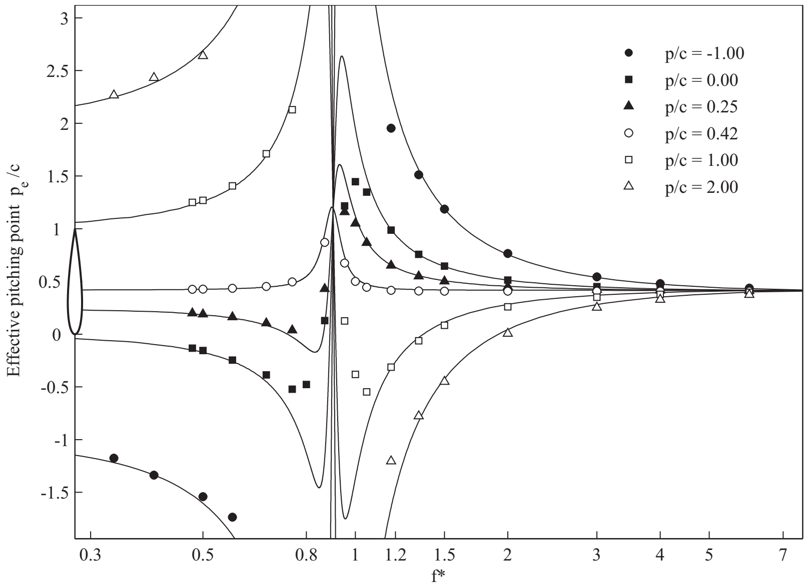

FIG. 18. Effective pitching point for the constant-density airfoil, shown for various pivot locations. Solid lines represent predictions from linear theory. At low values of frequency ratio, the effective pitching point tends towards the pivot location, while at high values of frequency ratio the effective pitching point approaches the airfoil's center of mass.

point p_e/c lies between 0.50 and 0.51 (essentially pitching at midchord), regardless of the specified center of mass. Additionally, if one calculates the airfoil's apparent angle of attack $\alpha(p,t)$, its maximum value $\alpha_{\max}$ is minimized at precisely this location, staying at almost zero (this is true only for $f^* = 1$). When pitching about the center of mass at the system's natural frequency, the passive heave motion allows the airfoil to face directly into the oncoming flow, resulting in minimal fluid forces and hence a very small net power input.

The result changes when we look at our constant-density airfoil, which does heave in part due to inertial forces. Unlike the previous configuration, where at $f^* = 1$ the airfoil essentially moves out of the way of the flow, when we pitch the airfoil about a point removed from its center of mass we find the complete opposite behavior. As we see in Fig. 12, the airfoil system with its center of mass fixed at the centroid produces maximum thrust near the spring system's natural frequency. In fact, experiments could not be conducted at $f^* = 1$ for most pitching locations because the fluid forces exceeded the limits of the force and torque transducer. Peak nondimensional power input occurs at a frequency ratio slightly under unity for all of the configurations tested, consistent with predictions from linear theory that place a maximum power coefficient around $f^* = 0.90$.

D. Characteristics of high-performance pitching

As we have seen, some of the best thrust and efficiency performance comes from configurations where the airfoil's center of mass is located at the centroid and the pivot point is at or behind the trailing edge. At first, this seems incongruous, since we have seen from static pitching tests that pivot points towards the trailing edge perform worse than pivot points towards the leading edge.

Figure 18, showing the effective pitching point for the fixed center-of-mass airfoil, provides an explanation why trailing-edge pivot locations produce the best propulsive performance with passive heave. At the frequency ratios where efficiency is maximized (f^* slightly greater than unity; see Fig. 13), the *trailing*-edge spring-mounted airfoil is moving in a way that most closely resembles pitching about a point ahead of the *leading* edge. The dynamics of having a center of mass removed

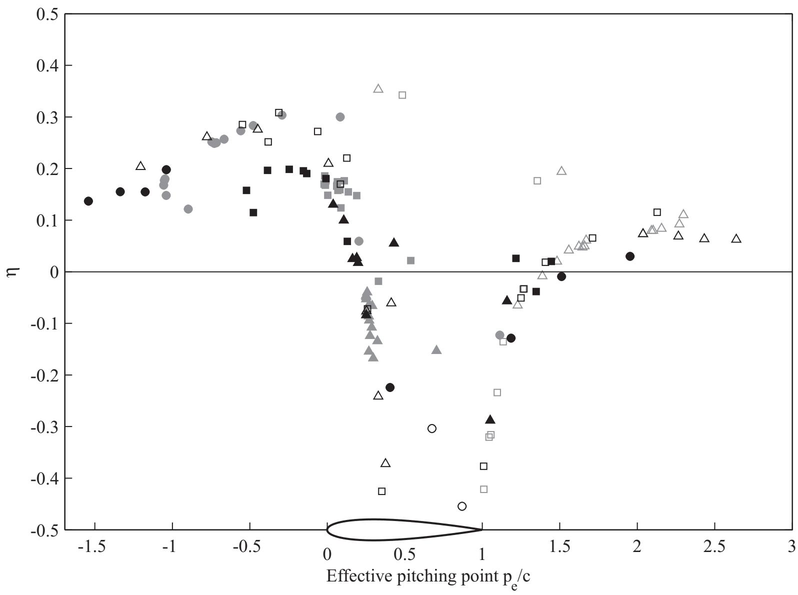

FIG. 19. Propulsive efficiency as a function of the nondimensional effective pitching location, shown for all experiments (the markers are consistent with Fig. 18). Gray symbols (open and closed) denote experiments with the unevenly weighted airfoil, and black symbols (open and closed) represent experiments with the constant-density airfoil.

from the pivot location cause the location of the effective pitching point to switch ends after a critical frequency ratio. This behavior is a general feature of the passive-spring dynamics and is present even without fluid forces.

If we plot the system's propulsive efficiency as a function of the effective pitching point, we arrive at the image shown in Fig. 19. Just as with the pure pitching case, propulsive efficiency is greatest for a pivot location in the vicinity or slightly ahead of the airfoil's leading edge. The addition of elastic heave, though, yields efficiencies that are much higher than those shown in Fig. 7. We can use this knowledge in combination with linear theory to validate good candidate parameters for efficient passive-heaving configurations.

A useful quantity for analyzing a pitching airfoil's performance is its effective angle of attack $\alpha(t)$. As the airfoil rotates and translates, the oncoming flow approaches it locally at an angle that can be significantly different than the pitch angle. Previous studies looking at the effect of angle of attack on flapping-foil propulsion, such as Read *et al.* [6], have employed predominantly heaving motion. Consequently their calculation of $\alpha(t)$ represents a single value for the entire airfoil, given by $\alpha(t) = \theta(t) - \arctan(\dot{y}/U_\infty)$. However, in our current study with strong pitching motion, the value $\dot{y}$ in the above equation (and hence the angle of attack) changes dramatically depending on where the heaving motion is measured. An example of this dependence is to consider $\alpha(t)$ for an airfoil undergoing pure pitching motion, but about a pivot point far upstream. If we simply take our measurement of $\dot{y}$ at the pivot point, we have $\alpha(t) = \theta(t)$. However, although the pivot point does not translate, the actual body of the airfoil is experiencing significant translation in the y direction. Therefore, we would be better served by taking our measurement of $\dot{y}$ at a point on the airfoil body, independent of the pivot location.

To define a precise location for measuring the angle of attack, we look back to the analysis of low-power pitching at $f^* = 1$. For the weighted airfoil operating at this frequency ratio, observations indicated that the airfoil was moving in a way that let it stay parallel with the local flow, evidenced by the fact that its net thrust was equivalent to that caused by its profile drag (also from visual

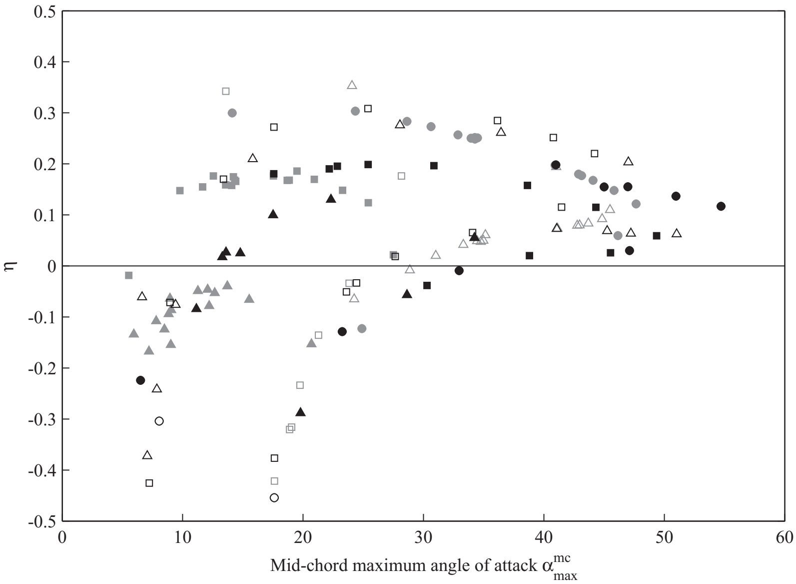

FIG. 20. Propulsive efficiency versus midchord maximum angle of attack for all passive pitching configurations. Gray symbols (open and closed) denote experiments with the unevenly weighted airfoil while black symbols (open and closed) represent experiments with the constant-density airfoil.

observations indicating a lack of a vortex wake behind the airfoil). We calculated the local angle of attack along the airfoil section and found that it was minimized at the half-chord point, a result that was consistent for all of the pivot locations tested. Therefore, we adopt the convention of evaluating the airfoil's angle of attack at its midchord point, denoting this value $\alpha^{mc}(t)$. We denote the maximum per-cycle value as $\alpha^{mc}_{\max}$; while the airfoil's maximum pitching angle θ_0 is the same for all experiments (8°), $\alpha^{mc}_{\max}$ varies widely across the different pitching configurations, reaching up to 55°.

Looking at Fig. 20, we find an interesting pattern in the distribution of propulsive efficiency versus peak midchord angle of attack. For many sets of experiments, the same value of $\alpha^{mc}_{\max}$ shows two distinct values of propulsive efficiency. This trend is consistent with an observation by Read *et al.* [6] that there is a bifurcation in defining the $\alpha_{\max}$ parameter; the same value of $\alpha_{\max}$ here can result from two different heave amplitudes. In terms of optimal performance, Fig. 20 shows no clearly defined peak in efficiency. However, we see that $\alpha^{mc}_{\max}$ is generally between 15° and 30° for individual airfoil configurations.

Another commonly used metric for oscillating airfoil performance is the Strouhal number based on the trailing edge excursion, $\mathrm{St}_A = fA/U_\infty$, where A is the vertical peak-to-peak distance traveled by the airfoil's trailing edge during one oscillation cycle. Figure 21 shows the airfoil's thrust and propulsive efficiency as a function of St_A for all experimental configurations.

While there is a reasonable correlation between the Strouhal number and thrust production, propulsive efficiency varies significantly. However, we find that peak propulsive efficiency generally occurs in the range of St_A between 0.15 and 0.35. This range is generally consistent with the results of previous studies of oscillating airfoil propulsion, such as Triantafyllou *et al.* [22] and Buchholz and Smits [4].

E. Extrapolating results to other pitching amplitudes and frequencies

To this point, all of the airfoil kinematics under consideration have maintained a fixed pitching amplitude of 8° and a reduced frequency k of two. How would our results change at different flapping amplitudes or frequencies?

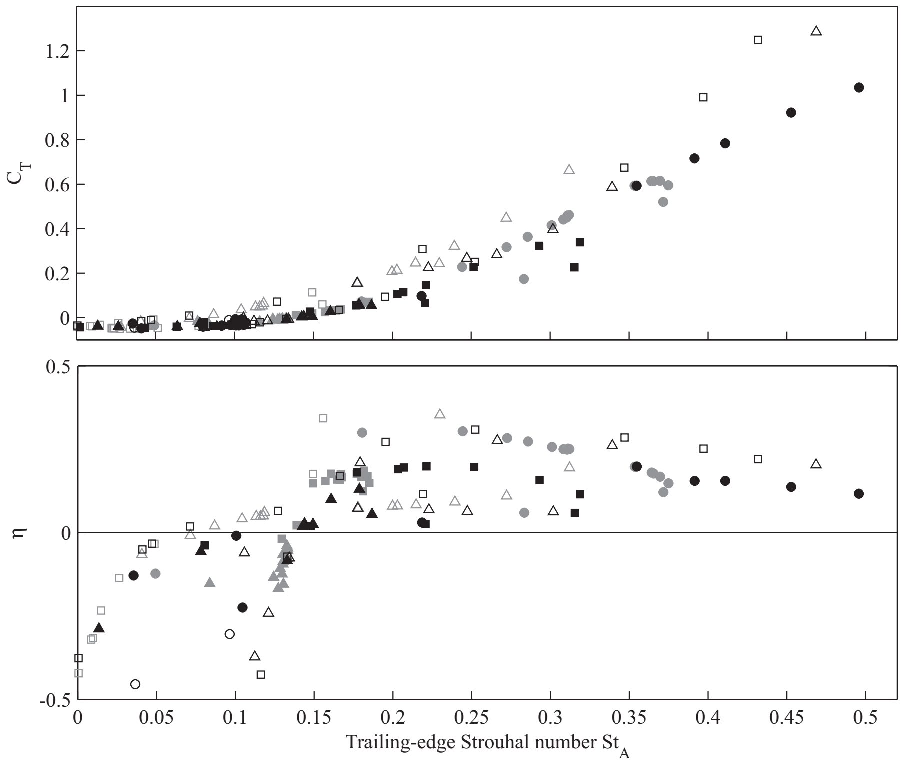

FIG. 21. Thrust and propulsive efficiency for all experiments as a function of the trailing-edge Strouhal number. Gray symbols (open and closed) denote experiments with the unevenly weighted airfoil while black symbols (open and closed) represent experiments with the constant-density airfoil.

In terms of pitching amplitude θ_0, we would expect similar behavior for other relatively small angles. Linear theory predicts that for pure pitching, propulsive efficiency is independent of pitching amplitude. Although the theory significantly overpredicts the magnitude of the airfoil's propulsive efficiency, we do not see significant change in its peak value below pitching amplitudes of about 8° [5]. At large values of pitching amplitude, experiments from the same study indicate that the airfoil's increased drag tends to outweigh its thrust production at reasonable oscillation frequencies. Large passive heaving motions would likely be required to produce a reasonable effective angle of attack and limit drag. On the other end of the scale, at smaller values of θ_0, it will be necessary to increase the pitching frequency in order to produce any meaningful thrust or efficiency; we can see from Fig. 21 that this requires generating a trailing-edge Strouhal number of at least about 0.15.

Modifying the airfoil's pitching frequency is slightly more complicated, at least with respect to the airfoil's pivot location. For a fixed pivot location, linear theory indicates that propulsive efficiency increases with pitching frequency. However, we know from experiments that optimal efficiency usually occurs in a particular range of Strouhal number. Therefore, if pitching frequency is decreased, we would expect that best efficiency would result from moving the pivot point further from the airfoil. Moving the pivot point away from the airfoil increases its trailing-edge motion amplitude, offsetting the reduction in Strouhal number due to decreasing the oscillation frequency.

We see experimental results for three different pitching frequencies in Fig. 22 for the case of pitching without heave. As expected, decreasing the reduced frequency from $k = 2$ to $k = 1$ moves the optimal pitching location further upstream from the airfoil's leading edge. The latter pitching frequency produces a maximum propulsive efficiency of 28%, though it does so with a very low

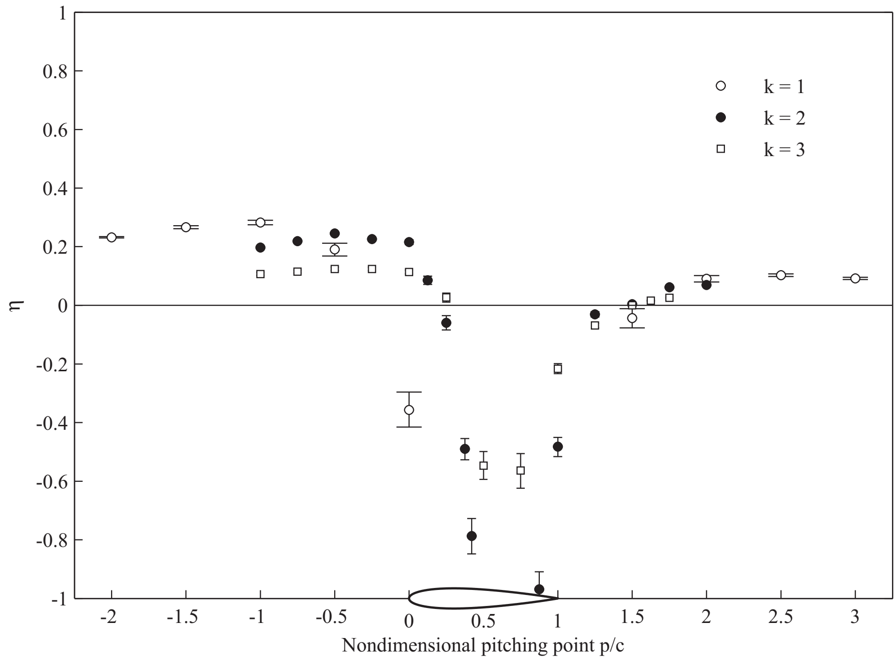

FIG. 22. Propulsive efficiency for an airfoil pitching without heave motion, plotted as a function of pivot location. Three reduced frequencies are shown; the pitching amplitude θ_0 for all cases is 8°.

amount of thrust ($C_T = 0.10$). Between reduced frequencies of two and three, there is a smaller change in the optimal pivot location, though the relative flatness of η versus p makes it difficult to determine this optimal location precisely.

Interestingly, there is a strong inverse trend between peak efficiency and the reduced frequency. Pitching quickly at $k = 3$ produces a best-case efficiency of only 12%. The aforementioned dependence of efficiency on trailing-edge Strouhal number helps explain this finding. For lower pitching frequencies, keeping the Strouhal number in the optimum range requires moving the pivot location further away from the airfoil's trailing edge. Pivoting about a point far removed from the airfoil body, in turn, produces kinematics that are more analogous to heaving motion. As heaving motion tends to be more efficient than pitching, we see a correspondingly higher value of propulsive efficiency. Conversely, when pivoting about a location interior to the airfoil body, its leading edge and trailing edge move in opposite directions, which we suspect causes strong leading-edge vortices that interfere with thrust production.

VII. CONCLUSIONS

We have used theoretical and experimental methods to explore the effect of elastic heaving motion on the propulsive qualities of an airfoil with controlled pitching. In the process, we have also examined the dependence of thrust generation and efficiency on the pivot location for a harmonically pitching airfoil.

For the case of a NACA 0012 airfoil section oscillating at a reduced frequency of 2 and a pitch amplitude of 8°, we find that passive heaving motion allows us to achieve propulsive efficiency reaching 35%, significantly larger than the maximum value of 25% possible with a static pivot. While this performance is still far behind that of fully articulated heaving-pitching motion, the boost in efficiency here requires no additional active actuation or control. Additionally, our results show that for the same value of efficiency, elastic heaving can more than double the amount of thrust produced over the rigid-pivot scenario.

We test two different types of airfoil dynamics, one with the airfoil's center of mass located at the pivot point and another with the center of mass independent of the pivot point. For the former case, inertial forces are unable to cause heaving motion; performing the experiments in air would show no y-direction translation. In the latter case, the airfoil's passive movement is the result of a combination of inertial forces and fluid forces. We find that this combination achieves better propulsive performance than when the passive motion is only influenced by fluid forces. Changing the distance between the pivot point and the center-of-mass location changes the amplitude and phase of the inertial force, which in turn influences the total heaving phase. Through this mechanism, one can tune the passive heaving motion to produce fluid dynamics that are better suited for propulsion.

Our results also explore the dynamics of allowing an airfoil with controlled pitching to translate freely in the heave direction (corresponding to a frequency ratio $f^* \to \infty$). We find that this arrangement generally does not improve the performance of the pitching airfoil. In one configuration, free heaving motion increased the airfoil's propulsive efficiency by five percentage points, but at the cost of decreased thrust.

Finally, we can examine the results of our passive-heave airfoil in the more general context of adding passive dynamics to airfoil propulsion. Previous research on airfoils with chordwise flexibility has shown that a moderate amount of compliance can improve peak performance, though too much flexibility is disadvantageous for airfoil propulsion. Our experimental results for a rigid airfoil with an elastic fixture mirror this conclusion. We also affirm results which indicate that although passive dynamics can significantly increase performance for a singly actuated airfoil, the resulting efficiency is still far below that achievable through independently controlled pitching and heaving motion.

ACKNOWLEDGMENT

This work was supported by the Air Force Office of Scientific Research under AFOSR award No. FA9550-11-1-0155, monitored by Dr. Douglas Smith.

[1] J. M. Anderson, K. Streitlien, D. S. Barrett, and M. S. Triantafyllou, Oscillating foils of high propulsive efficiency, J. Fluid Mech. **360**, 41 (1998).

[2] S. Heathcote and I. Gursul, Flexible flapping airfoil propulsion at low Reynolds numbers, AIAA J. **45**, 1066 (2007).

[3] M. A. Ashraf, J. Young, and J. C. S. Lai, Oscillation frequency and amplitude effects on plunging airfoil propulsion and flow periodicity, AIAA J. **50**, 2308 (2012).

[4] J. H. J. Buchholz and A. J. Smits, The wake structure and thrust performance of a rigid low-aspect-ratio pitching panel, J. Fluid Mech. **603**, 331 (2008).

[5] A. W. Mackowski and C. H. K. Williamson, Direct measurement of thrust and efficiency of an airfoil undergoing pure pitching, J. Fluid Mech. **765**, 524 (2015).

[6] D. A. Read, F. S. Hover, and M. S. Triantafyllou, Forces on oscillating foils for propulsion and maneuvering, J. Fluids Struct. **17**, 163 (2003).

[7] Q. Xiao and W. Liao, Numerical investigation of angle of attack profile on propulsion performance of an oscillating foil, Comput. Fluids **39**, 1366 (2010).

[8] W. McKinney and J. DeLaurier, Wingmill: An oscillating-wing windmill, AIAA J. Energy **5**, 109 (1981).

[9] J. M. Miao and M. H. Ho, Effect of flexure on aerodynamic propulsive efficiency of flapping flexible airfoil, J. Fluids Struct. **22**, 401 (2006).

[10] Q. Zhu, Numerical simulation of a flapping foil with chordwise or spanwise flexibility, AIAA J. **45**, 2448 (2007).

[11] E. R. Israeli, Simulations of a passively actuated oscillating airfoil using a discontinuous Galerkin method, Master's thesis, MIT, 2008.

[12] D.-w. Peng and M. Milano, Lift generation with optimal elastic pitching for a flapping plate, J. Fluid Mech. **717**, R1 (2013).

[13] M. M. Murray and L. E. Howle, Spring stiffness influence on an oscillating propulsor, J. Fluids Struct. **17**, 915 (2003).

[14] A. W. Mackowski and C. H. K. Williamson, Developing a cyber-physical fluid dynamics facility for fluid-structure interaction studies, J. Fluids Struct. **27**, 748 (2011).

[15] A. W. Mackowski and C. H. K. Williamson, An experimental investigation of vortex-induced vibration with nonlinear restoring forces, Phys. Fluids **25**, 087101 (2013).

[16] I. E. Garrick, *Propulsion of a Flapping and Oscillating Airfoil*, Report 567 (NACA, 1936).

[17] T. Theodorsen, *General Theory of Aerodynamic Instability And the Mechanism of Flutter*, Report 496 (NACA, 1935).

[18] T. von Kármán and J. M. Burgers, General aerodynamic theory: Perfect fluids, in *Aerodynamic Theory*, edited by W. F. Durand (Springer, Berlin, 1935), Vol. II.

[19] T. Theodorsen and I. E. Garrick, *Mechanism of Flutter: A Theoretical and Experimental Investigation of the Flutter Problem*, Report 685 (NACA, 1940).

[20] S. L. Brunton and C. W. Rowley, Empirical state-space representations for Theodorsen's lift model, J. Fluids Struct. **38**, 174 (2013).

[21] K. A. Harper, M. D. Berkemeier, and S. Grace, Modeling the dynamics of spring-driven oscillating-foil propulsion, IEEE J. Oceanic Eng. **23**, 285 (1998).

[22] G. S. Triantafyllou, M. S. Triantafyllou, and M. A. Grosenbaugh, Optimal thrust development in oscillating foils with application to fish propulsion, J. Fluids Struct. **7**, 205 (1993).

[23] M. J. Lighthill, Aquatic animal propulsion of high hydromechanical efficiency, J. Fluid Mech. **44**, 265 (1970).